RSC Chemical Biology

Accepted Manuscript

This article can be cited before page numbers have been issued, to do this please use: E. Puri, G. Biagiotti, J. Tricomi, J. Mravljak, S. Cicchi, M. Laurati, Y. van Kooyk, F. Chiodo, I. Urbancic, M. Anderluh and B. Richichi, *RSC Chem. Biol.*, 2025, DOI: 10.1039/D5CB00190K.

ROYAL SOCIETY OF CHEMISTRY

rsc.li/rsc-chembio

A nonavalent BODIPY with a multivalent arrangement of α-mannosides enables lectins recognition in fluorescence-based assays

Giacomo Biagiotti,[a,§] Edvin Purić,[b,§] Jacopo Tricomi,[a] Janez Mravljak,[b] Stefano Cicchi,[a] Marco Laurati,[a,f] Yvette van Kooyk,[c] Fabrizio Chiodo,[c,d] Iztok Urbančič,[e] Marko Anderluh,[b,*] Barbara Richichi[a,*]

[a]*Department of Chemistry 'Ugo Schiff', University of Firenze, Via della Lastruccia 3-13, 50019 Sesto Fiorentino, Italy*
[b]*Department of Pharmaceutical Chemistry, Faculty of Pharmacy, University of Ljubljana, Aškerčeva cesta 7, 1000 Ljubljana, Slovenia*
[c]*Department of Molecular Cell Biology and Immunology, Amsterdam UMC, Vrije Universiteit Amsterdam, Amsterdam 1081 HV, The Netherlands.*
[d]*Institute of Biomolecular Chemistry, National Research Council (CNR), via Campi Flegrei, 34, 80078 Pozzuoli, Naples, Italy.*
[e]*Laboratory of Biophysics, Condensed Matter Physics Department, Jožef Stefan Institute, Jamova Cesta 39, Ljubljana, Slovenia*
[f] *Consorzio per lo Sviluppo dei Sistemi a Grande Interfase, 50019 Sesto Fiorentino (FI), Firenze, Italy*
E-mail: barbara.richichi@unifi.it

Marko.Anderluh@ffa.uni-lj.si

§ G.B. and E.P. equally contributed to this work

Abstract

We report here on the use of the **Tris-BODIPY-OH** as a scaffold for the multivalent display of sugar heads. A chloroacetyl thioether ligation reaction easily yields to mannosylated BODIPYs, named **Man$_9$-BODIPY** and **(Man-TEG)$_9$-BODIPY**, which display nine mannose residues. Regardless of linker length, both glycoBODIPYs provide an arrangement of mannose heads that allows for proper recognition by the carbohydrate binding domain of Concanavalin A (ConA). Moreover, the interactions of **Man$_9$-BODIPY** with relevant human lectins, *i.e.* Dendritic cell-specific intercellular adhesion molecule-3-grabbing non-integrin (DC-SIGN) and Langerin, were further investigated. The approach proposed is versatile and paves the way for the development of multivalent and fluorescent glyco-BODIPY probes useful to interrogate carbohydrate-lectin interactions in different biological contexts.

View Article Online
DOI: 10.1039/D5CB00190K

Abbreviations

Concanavalin A (Con A), Dendritic cell-specific intercellular adhesion molecule-3-grabbing non-integrin (DC-SIGN), fluorescence polarization (FP), fluorescence correlation spectroscopy (FCS), fluorescence lifetime imaging microscopy (FLIM).

Keywords

BODIPY, C-type lectins, Concanavalin A, Langerin, DC-SIGN, fluorescence polarization assay, fluorescence correlation spectroscopy, fluorescence lifetime imaging microscopy, turbidimetry, carbohydrate-lectin interactions.

Introduction

Glyco-BODIPYs have emerged as a promising class of fluorescent and functional compounds that result from the integration of carbohydrates with BODIPY probes.[1,2] These conjugates exploit the synergic and favorable properties of both components which are assembled in post-functionalization reactions on pre-formed BODIPY cores using various chemistry (*i.e.* glycosidation reaction, click chemistry and amide/ester formation) or by the introduction of carbohydrate motifs during BODIPY core synthesis.

The BODIPY core provides robust and tunable optical properties, while the carbohydrate moieties serve to improve water solubility, increase biocompatibility, reduce cytotoxicity, and further act as molecular recognition units enabling specific biological targeting. Moreover, the chemical flexibility of both BODIPY core and carbohydrate structures opens new avenues for designing multifunctional probes for specific applications *e.g.* targeted imaging and therapeutic interventions. Accordingly, the mutual benefit of this integration resulted in fluorescent glycoconjugates which served in bioimaging applications to get key insights on the trafficking of glycans[1–5] or related lectins. Likewise, saccharides were included as structural recognition elements of the probe for the targeting of specific lectins in various immune and cancer settings.[1,2,6–9]

The clustering of glycans within the glycocalyx has inspired glycoscientists to develop structurally different scaffolds able to provide the multivalent display of sugar residues thus improving the avidity of the binding to the lectins.[10–20] Recently, some BODIPY cores served as scaffolds for the conjugation of multiple copies of sugar heads resulting in improved lectin-mediated cell uptake by means of multivalent binding interactions with the biological targets.[1] The availability of an affordable and high fluorescent BODIPY with a core that can be easily functionalized is crucial for the development of advanced and multifunctional

View Article Online
DOI: 10.1039/D5CB00190K

BODIPY-based architectures that can provide the multivalent display of sugar heads to a single BODIPY core.

In this context, we have recently described the synthesis of the water-soluble **Tris-BODIPY-OH** (**Figure 1**)[21] that contains nine hydroxyl groups at the edges of the BODIPY core, and we demonstrated that it is a biocompatible probe both *in vitro* and *in vivo* applications. In this work, we decided to investigate its potential as a multivalent and fluorescent platform for the display of multiple copies of sugars. Accordingly, we set out to explore the integration of sugar heads into the **Tris-BODIPY-OH** aiming to develop a multifunctional and modular molecular tool. In particular, D-mannose was selected as sample sugar head for our study. Moreover, the intrinsic optical properties of **Tris-BODIPY-OH** facilitates the study of the sugar heads arrangement on the BODIPY core and thus the biomolecular recognition with lectins using comparative fluorescence-based assays.

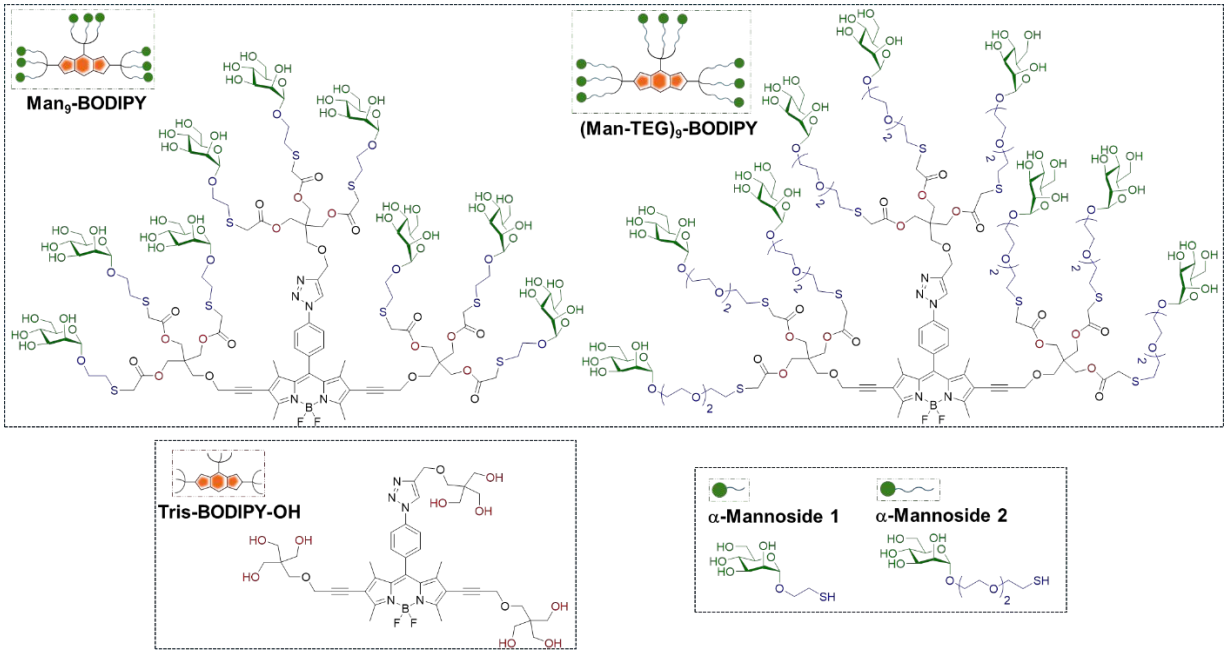

Figure 1. Structures and schematic representations of **Tris-BODIPY-OH**, α-Mannosides **1** and **2** used in this work, **Man$_9$-BODIPY** and **(Man-TEG)$_9$-BODIPY**.

The **Tris-BODIPY-OH** was combined with two suitable functionalized α-mannosides (compounds **1** and **2**,[22,23] **Figure 1**) which differ for the length of the linker at the anomeric position of the mannose. It resulted in two mannosylated BODIPYs, named **Man$_9$-BODIPY** and **(Man-TEG)$_9$-BODIPY** (**Figure 1**), which display nine mannose residues conjugated to

View Article Online
DOI: 10.1039/D5CB00190K

the BODIPY scaffold. Accordingly, we report here on the design and synthesis of **Man$_9$-BODIPY** and **(Man-TEG)$_9$-BODIPY**, and a preliminary screening using the plant mannose-binding lectin Concanavalin A (Con A). Then, the investigation of the binding of **Man$_9$-BODIPY** to two relevant human lectins, *i.e.* Dendritic cell-specific intercellular adhesion molecule-3-grabbing non-integrin (DC-SIGN) and Langerin, was further performed.

Thanks to the intrinsic fluorescence properties of the core, **Man$_9$-BODIPY** proved to be an efficient tool and facilitated the study of carbohydrate-lectin interactions using different and comparative fluorescence-based assays *i.e.* a fluorescence lifetime imaging microscopy (FLIM), a fluorescence polarization (FP) assay, and a fluorescence correlation spectroscopy (FCS).

Results and discussion

Synthesis, optical characterization and agglutination studies of Man$_9$-BODIPY and (Man-TEG)$_9$-BODIPY.

The chloroacetyl thioether (ClAc) ligation[24,25] was selected as a synthetic strategy for the assembly of **Man$_9$-BODIPY** and **(Man-TEG)$_9$-BODIPY**. In particular, **Tris-BODIPY-OH** (**Scheme 1**) and the α-mannoside **1**, bearing a thiol-ending spacer at the anomeric carbon, were synthesized accordingly with previously reported protocols.[21–23] Then, the α-mannoside **1** was used as a crude mixture in the coupling reaction (see ESI). The α-mannoside **2** bearing, at the anomeric carbon, a tetraethylene glycol (TEG) spacer with a terminal thioacetate group was prepared using the imidate **3**[26] (**Scheme 1**), as glycosyl donor, and the acceptor **4**[27] in a glycosidation reaction with trimethylsilyl trifluoromethanesulfonate (see ESI) to afford the protected derivative **5**. Then, the hydrolysis of acetate groups in basic conditions, and subsequent treatment of the crude with tributylphosphine afforded the α-mannoside **2** which was used as a crude mixture in the coupling reaction (see ESI).

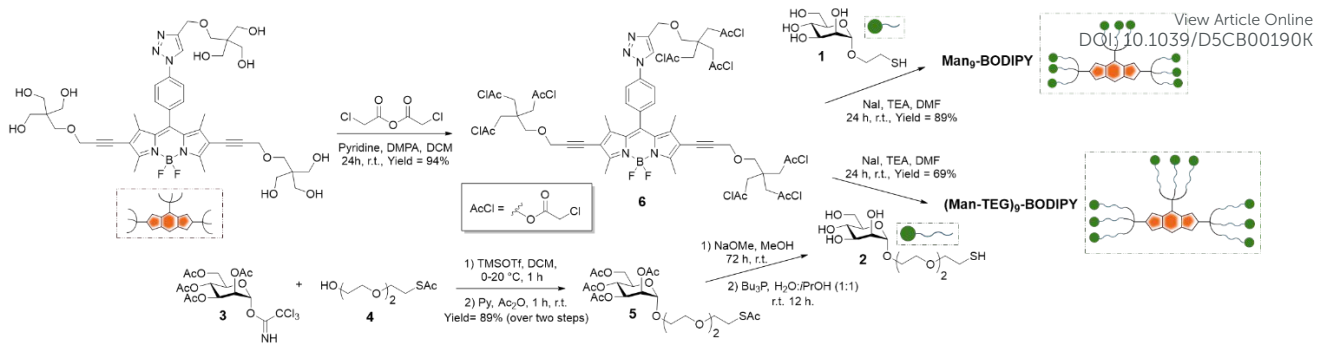

Scheme 1. Synthesis of **Man$_9$-BODIPY** and **(Man-TEG)$_9$-BODIPY**.

The nine hydroxyl groups of **Tris-BODIPY-OH** were reacted with chloroacetic anhydride to afford compound **6** in high yield (94%). The chloroacetyl thiols ligation reactions between **Tris-BODIPY-OH** and the α-mannosides **1** and **2** were performed in dry dimethylformamide (DMF) in presence of an excess of sodium iodide (NaI). The nonavalent glycoBODIPYs **Man$_9$-BODIPY** and **(Man-TEG)$_9$-BODIPY** were purified by subsequent trituration protocols with organic solvents (see experimental), and then dialysis *vs* water (membrane cut-off 1000 Da). Accordingly, **Man$_9$-BODIPY** and **(Man-TEG)$_9$-BODIPY** were isolated in good yield (89% and 69% respectively) and analyzed by HPLC-MS and NMR spectroscopy (see ESI, **Figures S1-S10**). Next, the photochemical properties of **Man$_9$-BODIPY** and **(Man-TEG)$_9$-BODIPY** were evaluated (**Figure 2** and see ESI **Figures S11-12**).

View Article Online
DOI: 10.1039/D5CB00190K

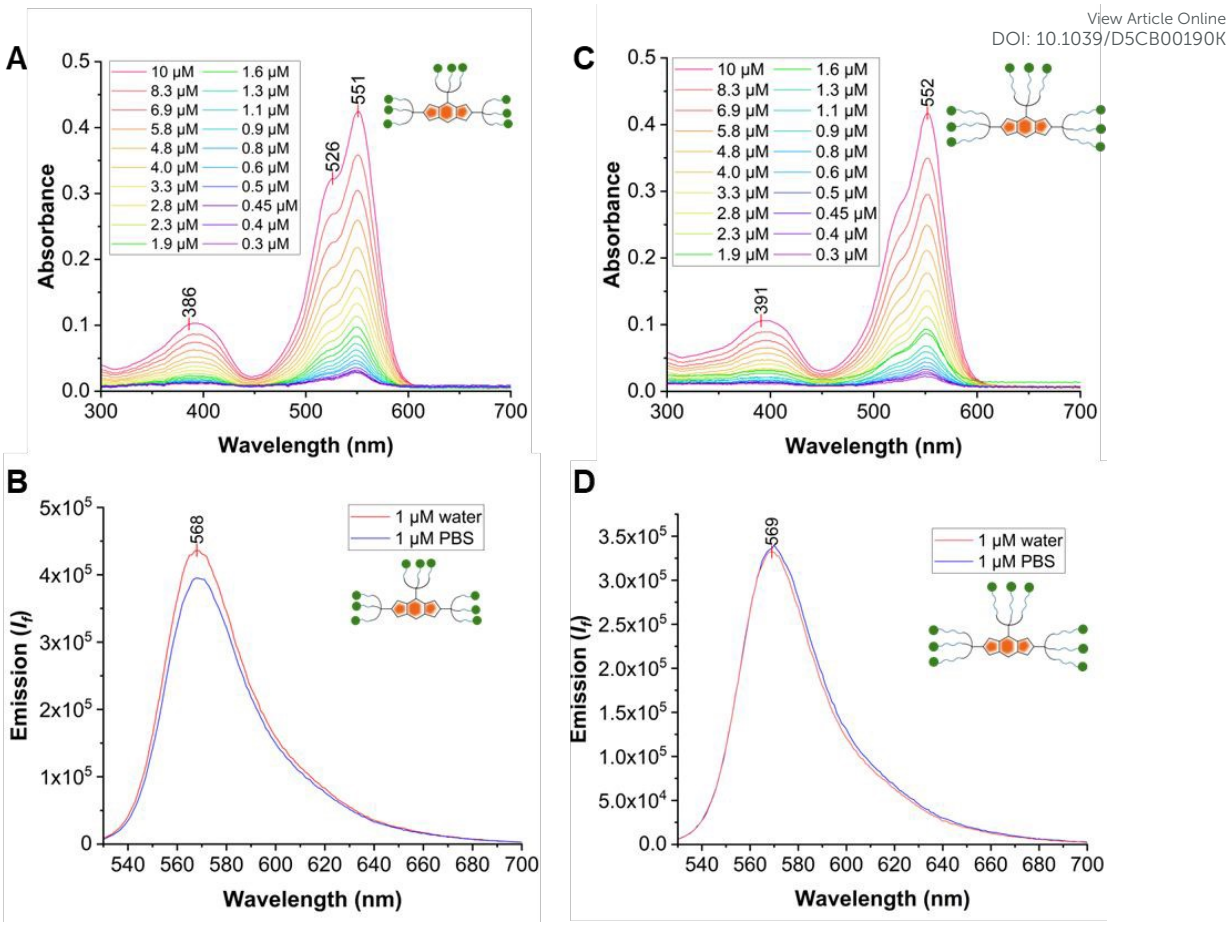

Figure 2. A: Absorbance spectra of **Man$_9$-BODIPY** in water at different concentrations (0.3 -10 μM); **B**: Emission spectra of **Man$_9$-BODIPY** (1 μM in water, and PBS pH = 7.4) after excitation at 520 nm; **C**: Absorbance spectra of **(Man-TEG)$_9$-BODIPY** in water at different concentrations (0.3 -10 μM); **D**: Emission spectra of **(Man-TEG)$_9$-BODIPY** (1 μM in water, and PBS pH = 7.4) after excitation at 520 nm

In particular, the UV–vis absorption spectra were recorded in water, and resulted in a similar absorption pattern previously reported for the **Tris-BODIPY-OH**,[21] with main absorption peaks around λ = 551 nm (see ESI, **Figures 2A** and **2C**) assigned to the transition S0 → S1, and high molar extinction coefficients (4.1 x 10^4 $M^{-1}cm^{-1}$, see ESI, **Figures S11-12**). Upon excitation at 520 nm, emission spectra in both PBS and water showed emission peaks centered around 568 nm (see ESI, **Figures 2B** and **2D**).

Concanavalin A (ConA) was selected as model of mannose-binding lectin[18] to study if the arrangement of the mannose residues allowed for proper recognition by lectins' carbohydrate binding domain. Accordingly, preliminary agglutination experiments were performed by following a previously reported protocol,[28] thus expecting aggregation of the

View Article Online
DOI: 10.1039/D5CB00190K

lectin with the mannosylated BODIPYs driven by the molecular recognition of the mannose residues on the fluorescent probes. Accordingly, the **Tris-BODIPY-OH** was used as a negative control. The changes in absorption (λ = 490 nm) of the solutions of the glycoBODIPYs treated with a fixed concentration of ConA (20μM in HEPES 25 mM, pH 7.6, 1 mM $CaCl_2$, 1 mM $MnCl_2$) was monitored over time (0-30 min, **Figure 3A**).

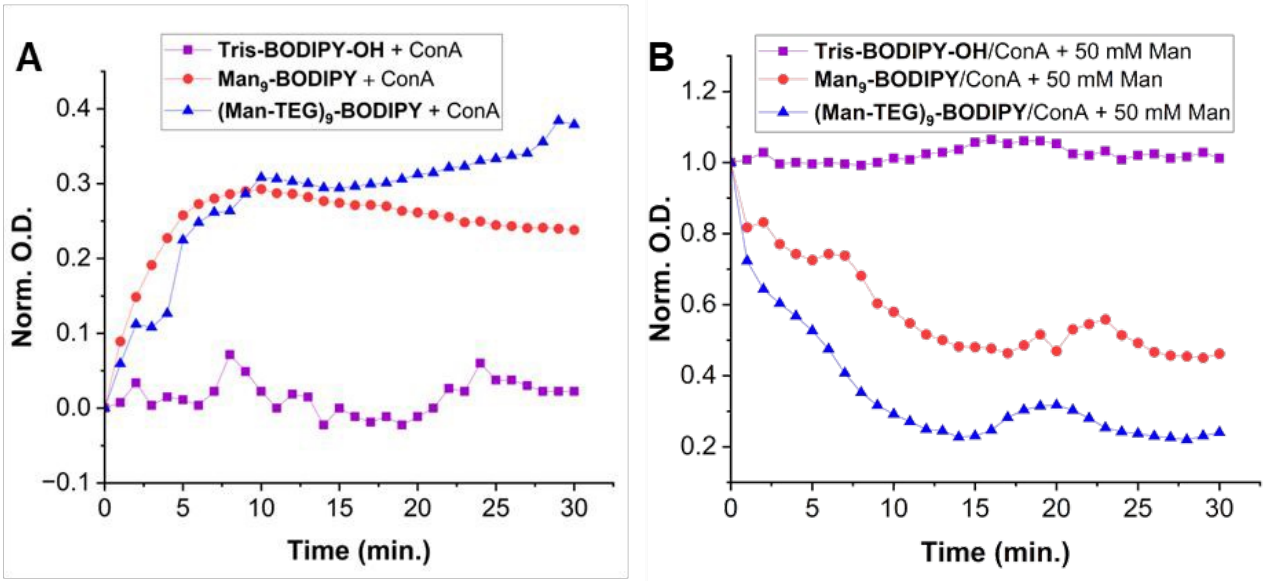

Figure 3. Turbidimetry analysis. **A**: absorbance (λ = 490 nm) changes over time of a solution (20 μM) of **Tris-BODIPY-OH** (purple line), **Man_9-BODIPY** (red line), and **$(Man\text{-}TEG)_9$-BODIPY** (blue line) treated with a solution of ConA (20 μM in HEPES 25 mM, pH = 7,6, 1 mM $CaCl_2$, 1 mM $MnCl_2$); **B**: deagglutination over time of glycoBODIPYs/ConA by treatment with a solution of α-*O*-methyl-D-mannopyranoside (50 mM).

Data obtained indicated that the turbidity of the solutions of both glycoBODIPYs increased over time (**Figure 3A**, blue and red lines). Moreover, the addition of a solution of α-*O*-methyl-D-mannopyranoside (50 mM) resulted in a fast deagglutination process with a decrease of the turbidity of the solutions (**Figure 3B,** blue and red lines). No change in the absorption was observed in the mixture **Tris-BODIPY-OH**/ConA (**Figure 3A**, purple line). Altogether, these data confirmed that the aggregation was a consequence of the recognition of the mannose residues on the BODIPYs.

View Article Online
DOI: 10.1039/D5CB00190K

Man_9-BODIPY is a useful probe in fluorescence-based assays: fluorescence lifetime imaging microscopy (FLIM), fluorescent polarization (FP) assay and fluorescent correlation spectroscopy (FCS).

Fluorescence lifetime imaging microscopy (FLIM)[29] is a widely applied and impactful technique that has the capability of revealing changes in the molecular environment of fluorescent dyes. Such changes, that are not evidenced by other spectral techniques, are detected through measurement of the lifetime of a fluorophore in an excited state before it decays to a less energetic state by emitting a photon. FLIM is successfully applied to investigate interactions at the intermolecular level, conformations of proteins and concentrations of analytes, among others. Accordingly, FLIM was used in this work to directly visualize the formation of the glycoBODIPY/ConA complexes. **Figure 4** shows FLIM images of the (free) BODIPY solutions (left panels) and in the presence of ConA (right panels). The color scale in the images corresponds to the dye lifetime measured by FLIM for each pixel in the image. As expected, the dye distribution and the lifetime distribution are essentially uniform in the free dyes. One can notice a slight shift of the color of the **Man_9-BODIPY** towards green/yellow, indicating a longer lifetime. This is confirmed by the histograms of detected lifetimes (see ESI, **Figure S13**) for all the three BODIPYs. In the presence of ConA, a clear difference between **Tris-BODIPY-OH** and the mannosylated BODIPYs is observed. While for **Tris-BODIPY-OH** the distributions of dye and lifetime are still uniform, for the mannosylated BODIPYs we observe the presence of ConA aggregates and fluorescence lifetimes clearly shifted towards green/yellow, *i.e.* longer lifetimes. This finding is again quantitatively confirmed by the lifetime histograms (see ESI, **Figure S13**): for **Tris-BODIPY-OH**, the peak of the histogram is unchanged and one observes only a broadening, for the mannosylated BODIPYs the entire histogram is shifted to longer lifetimes, as an effect of the formation of the complex. It should be noted that the lifetime histograms for **Man_9-BODIPY** and **$(Man\text{-}TEG)_9$-BODIPY** are essentially comparable in presence of ConA (see ESI, **Figure S13**).

View Article Online
DOI: 10.1039/D5CB00190K

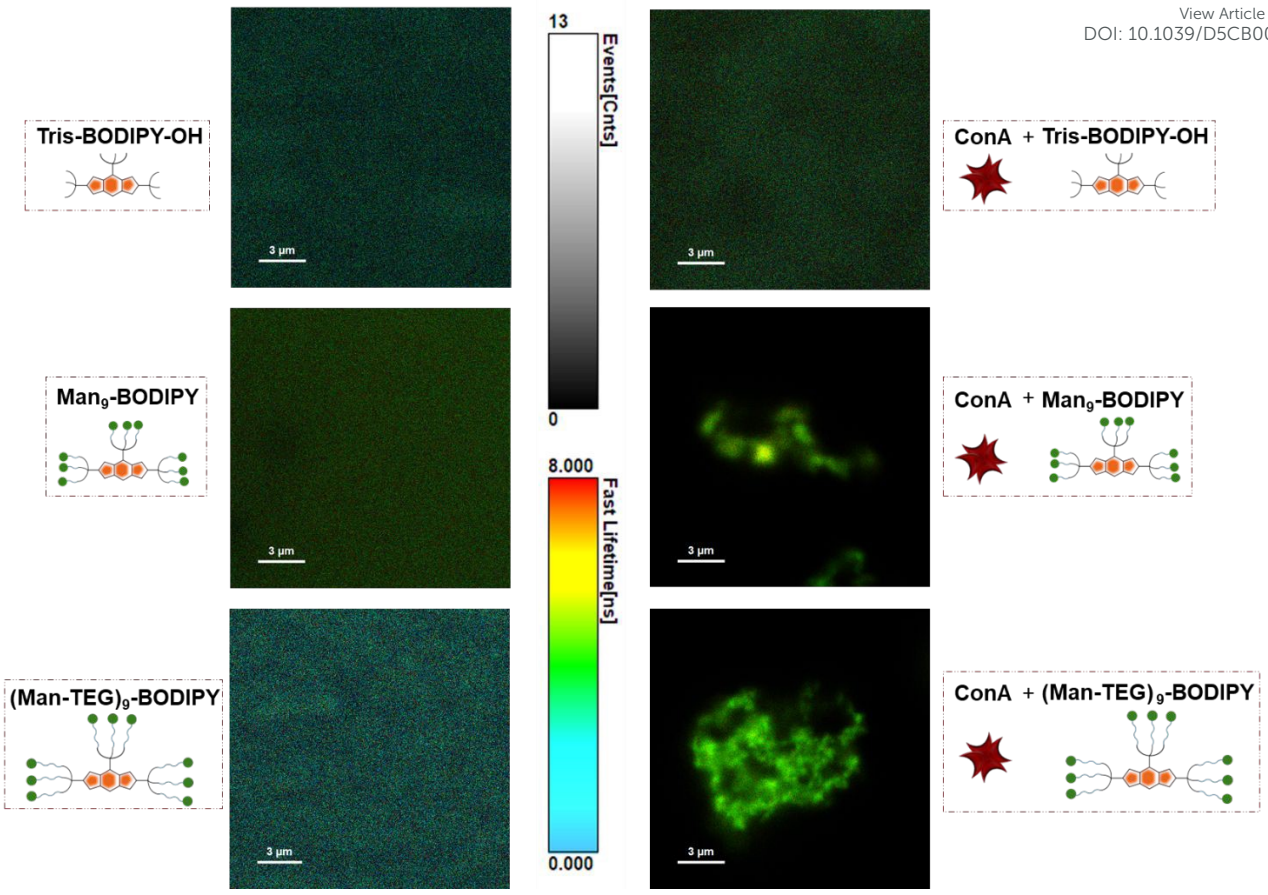

Figure 4. FLIM images measured for: (Left panels) the (free) BODIPY solutions 500 nM in HEPES 25 mM pH 7.6, 1 mM $CaCl_2$, 1 mM $MnCl_2$ and for (Right panels) solutions of the BODIPYs (500 nM) combined with ConA (500 nM in HEPES 25 mM pH 7.6, 1 mM $CaCl_2$, 1 mM $MnCl_2$). The gray scale-bar represents the number of photon events counted for pixel, while the color scale-bar represents the measured lifetime.

Fluorescence polarization (FP) is a widely used technique in biochemical and medicinal chemistry research for studying ligand-protein interactions, protein-protein interactions and antigen-antibody interactions. Major advantage of FP over similar methods is that it enables real-time measurements in solution, it does not require target protein manipulation (immobilization to a chip or on microtiter plates), thus it is an excellent method for screening compound libraries in a high-throughput protocol.[30] One of the most critical aspects of the FP assay is the requirement for a fluorescent probe with both high quantum yield and high photostability,[30] properties that both glycoBODIPYs, **Man_9-BODIPY** and **$(Man\text{-}TEG)_9$-BODIPY**, exhibit. Furthermore, the probe should exhibit selective binding based on the "ligand" part rather than the fluorescent moiety. Accordingly, the binding

View Article Online
DOI: 10.1039/D5CB00190K

properties of **Man_9-BODIPY** and **$(Man\text{-}TEG)_9$-BODIPY** with ConA, were evaluated in a FP assay.[18] **Tris-BODIPY-OH** was used as negative control to confirm that the fluorescent moiety alone does not promote nonspecific binding. In three separate experiments, a fixed concentration of BODIPYs was incubated with increasing concentrations of ConA. As expected, **Tris-BODIPY-OH** did not bind to ConA (**Figure 5A,** see ESI **Figure S14A**).

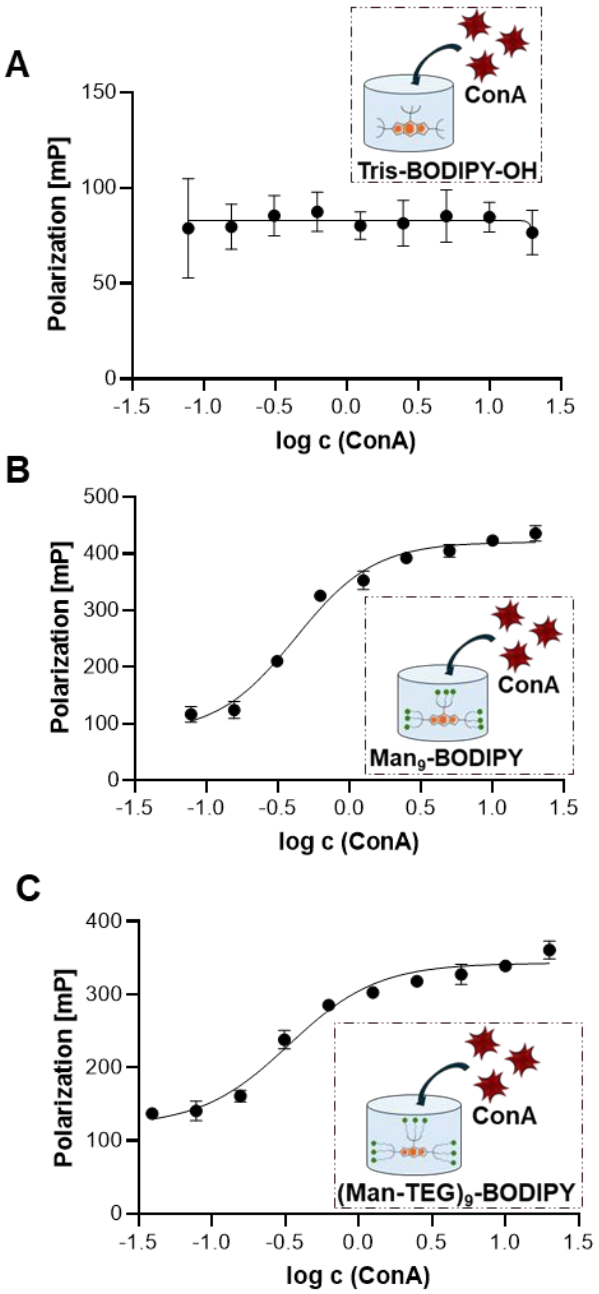

Figure 5. Binding of ConA to **Tris-BODIPY-OH** (**A**), **Man_9-BODIPY** (**B**), and **$(Man\text{-}TEG)_9$-BODIPY** (**C**). A fixed concentration of the fluorescent probes (0.5 μM) was mixed with a range of increasing concentrations of Con A (X-axis), and fluorescence polarization was

View Article Online
DOI: 10.1039/D5CB00190K

measured (Y-axis). The following settings were used for the FP assay: λ_{ex} =520/15 nm and λ_{em}=555/15 nm, calibrated G-factor for BODIPYs. All experiments were conducted at 25 °C.

Conversely, a dose-dependent increase of fluorescence polarization was observed in the titration experiments of ConA with **Man$_9$-BODIPY** (**Figure 5B**, see ESI **Figure S14B**) and with **(Man-TEG)$_9$-BODIPY** (**Figure 5C**, see ESI **Figure S14C**). The experiment also showed a high binding affinity for both mannosylated BODIPYs, which is due to the multivalent display of the mannose heads on the BODIPY core. K_d values in the nanomolar range (see ESI, **Table S1**, 300 nM for **Man$_9$-BODIPY** and of 120 nM for **(Man-TEG)$_9$-BODIPY**) were observed for the binding of the glycoBODIPYs to ConA. Altogether these data indicated that the length of the linker had a minor and barely significant effect on the recognition of the mannose residues by the carbohydrate recognition domains of the lectin. Accordingly, looking at the differences observed in the lifetime of the two glycoBODIPY probes in their unbound (free) state (see ESI **Figure S13**), we decided to proceed further with the investigations with **Man$_9$-BODIPY**, which is the probe that showed the highest lifetime values and longer-lived excited states may indicate more photostable or less environmentally sensitive fluorophores.

Titration experiments allowed us to define the concentration of ConA to be used in a competitive displacement assay, which was set to 2 μM. To further evaluate to possibility to use this glycoBODIPY probe in a competitive test, we investigated the ability of **Man$_9$-BODIPY** to be efficiently displaced by a potential lectin-binding ligand. Accordingly, **Man$_9$-BODIPY** was used in a competitive setting with D-mannose as lectin-binding ligand (**Figure 6**).

View Article Online
DOI: 10.1039/D5CB00190K

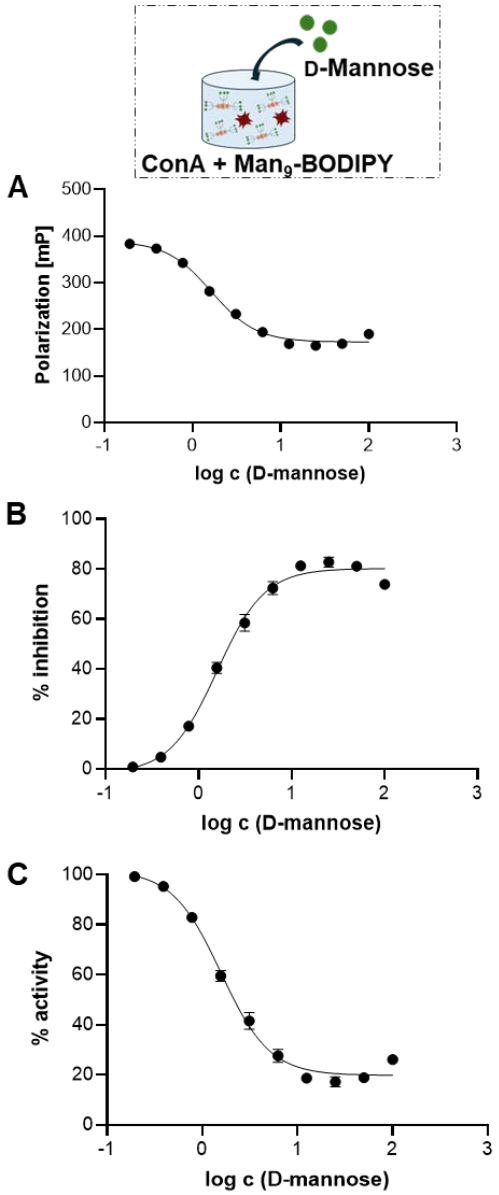

Figure 6. Binding curves (**A**, **B**, **C**) of the competitive FP assays using fixed concentrations of **Man$_9$-BODIPY** (0.5 μM) and ConA (2 μM) and adding increasing concentrations of D-mannose. The fluorescence polarization is expressed in millipolarization (mP) units (**A**). The relationship between relative inhibition (%, **B**), activity (%, **C**) and log c (D-mannose) is also shown. Relative inhibition refers to competitive inhibition of **Man$_9$-BODIPY** binding to ConA normalised to maximum absolute inhibition achieved, while relative activity refers to the values describing relative **Man$_9$-BODIPY** binding to ConA.

A solution of Con A was thus treated with a fixed concentration of **Man$_9$-BODIPY** and then changes in the fluorescence polarization according to the addition of a range of increasing concentrations of D-mannose were analysed. Binding curves and binding

View Article Online
DOI: 10.1039/D5CB00190K

properties of D-mannose are showed in **Figure 6** (see also ESI, **Figure S15**). The addition of D-mannose resulted in a dose-dependent reduction of the observed fluorescence polarization proving that D-mannose competitively displaced the probe (**Figure 6A**). Accordingly, K_d value of D-mannose resulted in 1.35 mM (see ESI, **Table S2**), which is in line with previously reported values.[31,32]

Then, fluorescence correlation spectroscopy (FCS) was used as comparative technique to further support our data. FCS reports on differences in translational diffusion[33,34] rather than rotational diffusion in polarization experiments described above. Accordingly, the binding of **Tris-BODIPY-OH** and **Man$_9$-BODIPY** to ConA was evaluated. **Figure 7** shows fluorescence autocorrelation curves for both probes. Without the protein (ConA) a slight shift of curve towards longer lag times was observed for **Man$_9$-BODIPY**, as a consequence of the slower diffusion compared to **Tris-BODIPY-OH** (**Figure 7A**).

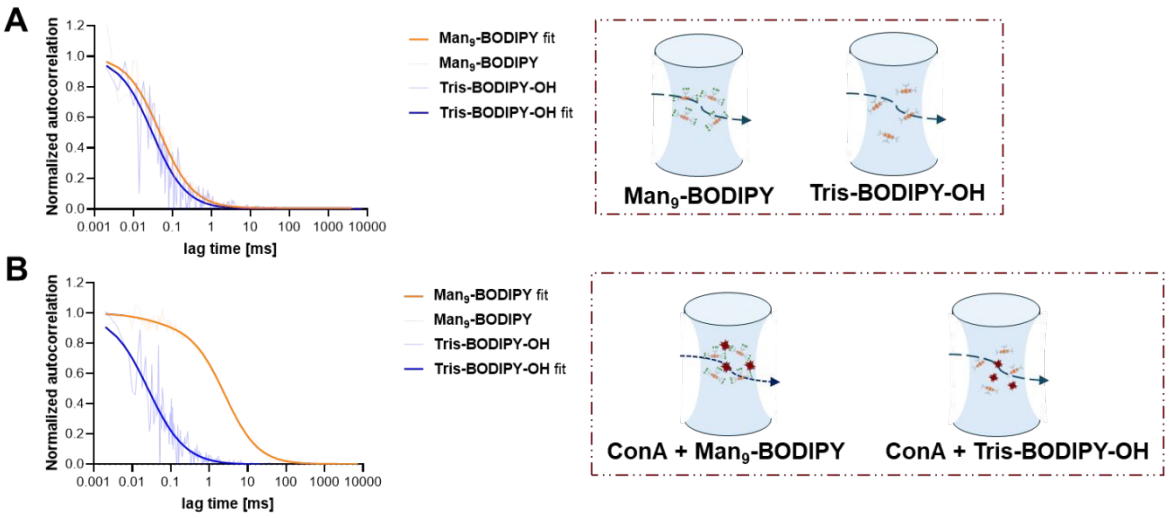

Figure 7. Fluorescence autocorrelation curves for both probes (**Man$_9$-BODIPY** and **Tris-BODIPY-OH**, colours as indicated in the legend) in absence (**A**) and presence (**B**) of ConA, where the right-shifted curve for **Man$_9$-BODIPY** (orange) indicates a slow-down in diffusion of the probe due to binding to the protein. The light thin lines represent the correlated data, while the smooth curves correspond to the fits by a 3D-diffusion model.

This is in line with the higher molecular weight of the mannosylated BODIPY compared to its non-glycosylated precursor **Tris-BODIPY-OH**. In the presence of ConA, the pronounced right-shift of curve for **Man$_9$-BODIPY** indicates an approximately 50-fold slow-

View Article Online
DOI: 10.1039/D5CB00190K

down of the diffusion rate (**Figure 7B** and see ESI, **Figure S16**), which independently confirms probe's multivalent binding to the ConA ((monovalent attachment of a roughly 2-kDa probe to a 100-kDa globular protein should result in approx. 4-fold slow-down). Conversely, no shift was observed when **Tris-BODIPY-OH** was exposed to ConA.

To further validate the robustness of our study and the possibility to study the carbohydrate-lectin interactions of **Man_9-BODIPY** with other lectins, we decided to include in this study two relevant human lectins. The molecular and immunological cross-talk between the host and the environment (from pathogens to the tumor microenvironment) is mostly driven by carbohydrate-mediated interactions. Most of the antigen-presenting cells are equipped by a library of pattern recognition receptors able to sense and recognize damage-associated molecular patterns. Among the pattern recognition receptors, lectins are conserved receptors able to module innate immune responses. In particular, DC-SIGN and Langerin are two important C-type lectins involved in several immuno-modulatory phenomena.[35,36] These lectins are known to recognize mannose residues and thus they were selected as model human lectins and included in this study.

DC-SIGN and Langerin chimera lectins[37,38] were used in this study. Due to their lower availability of such lectins compared to ConA, titrations were performed using fixed concentrations of Langerin (**Figure 8A**) or DC-SIGN (**Figure 8B**) lectins, with increasing concentrations of the **Man_9-BODIPY** added in two separate titration experiments (**Figure 8**, **Table 1**, and see ESI **Figure S17**).

Table 1. Binding properties of **Man_9-BODIPY** against Con A, Langerin and DC-SIGN.

	Con A	**Langerin**	**DC-SIGN**
K_d [μM]	0.30 ± 0.04	0.20 ± 0.01	0.33 ± 0.08
mP_{max} [mP]	439 ± 27	413 ± 14	541 ± 54
mP_0 [mP]	93.3 ± 12.9	73.7 ± 2.8	76.7 ± 6.2

View Article Online
DOI: 10.1039/D5CB00190K

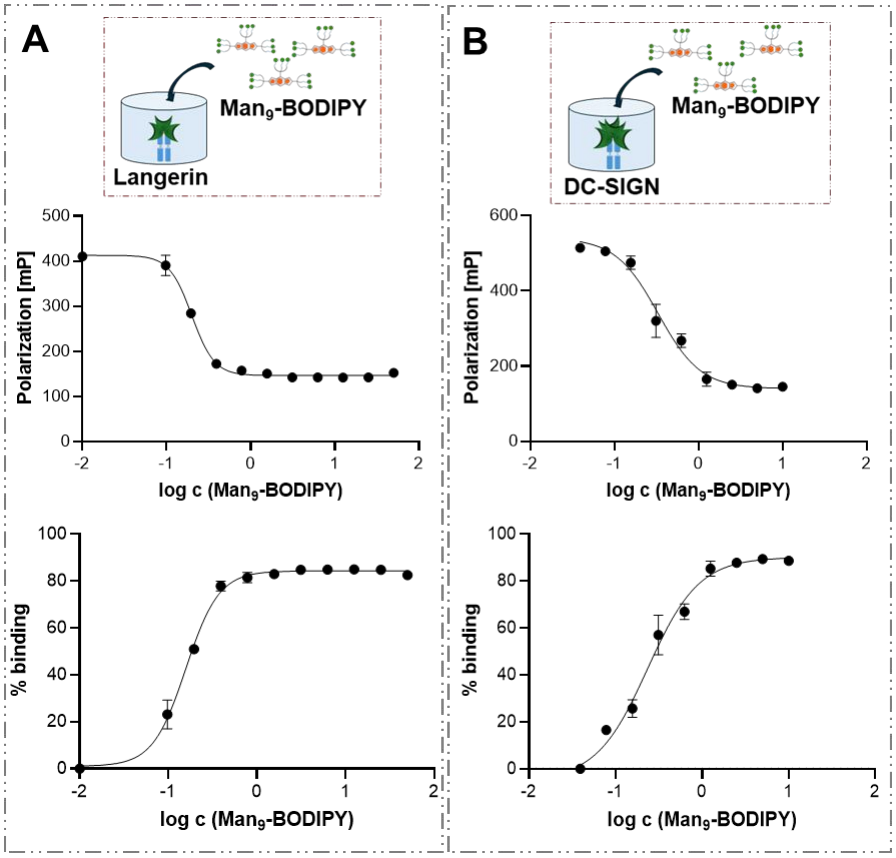

Figure 8. (**A**) Binding of Langerin to **Man$_9$-BODIPY**. A fixed concentration of Langerin (0.5 µM) was mixed with a range of concentrations of **Man$_9$-BODIPY** (X-axis), and fluorescence polarization was measured (Y-axis). (**B**) Binding of DC-SIGN to **Man$_9$-BODIPY**. A fixed concentration of DC-SIGN (0.05 µM) was mixed with a range of concentrations of **Man$_9$-BODIPY** (X-axis), and fluorescence polarization was measured (Y-axis).

Using the FP assay, the interaction between the mannose residues of **Man$_9$-BODIPY** and the target lectins was successfully analyzed. In this case, the binding curve is inverted compared to that in **Figure 8B**, as increasing the probe concentration leads to a higher fraction of free probe, which depolarizes the light. Specifically, **Man$_9$-BODIPY** displayed binding affinities (K_d values) in the nanomolar range for both C-type lectins 330 nM for DC-SIGN and and 200 nM for Langerin. Overall, these data demonstrate that **Man$_9$-BODIPY** arranges the sugar heads on the BODIPY core in a way that facilitates the recognition by the carbohydrate-binding domains of the three different lectins.

View Article Online
DOI: 10.1039/D5CB00190K

Conclusions

We report here on the use of the BODIPY dye as a scaffold for the multivalent display of sugar heads. The resulting **Man_9-BODIPY** exhibited a nanomolar affinity towards the studied lectins due to the clustering of the sugar heads on the BODIPY core, proving to be a valuable tool for studying carbohydrate-lectin interactions in two comparative fluorescence-based assays. Notably, glycosides containing a thiol-ending spacer at the anomeric position are readily available. Accordingly, using the chloroacetyl thioether ligation reaction as a synthetic strategy to conjugate nine copies of α-mannosides demonstrates the versatility of this approach which was used to prepare two glycoBODIPYs with different linkers. Indeed, this makes the **Tris-BODIPY-OH** a universal scaffold for the conjugation of other sugar heads or glycomimetics, thus expanding the range of applications of the resulting glycosylated BODIPY-probes. Combining the multivalent presentation of sugar heads with the intrinsic fluorescence properties of the BODIPY enables the development of glycosylated fluorescent tools with an improved affinity for target lectins[39]. These tools can be useful for studying lectin trafficking *in vitro* or *in vivo* settings, or for bioimaging and therapeutic applications in the context of pathogen-derived biofilms.[40]

Experimental

Materials and methods. All reagents, whose synthesis is not described, were commercially available and were used without any further purification, if not specified otherwise. ConA was purchased from Sigma Aldrich (L7647-100MG). NMR spectra were recorded on Varian Inova 400, Mercury plus 400 and Gemini 200 instruments. Chemical shifts were reported in parts per million (ppm) relative to the residual solvent peak rounded to the nearest 0.01 for proton and 0.1 for carbon (reference: $CHCl_3$ [1H: 7.26 ppm, 13 C: 77.0 ppm]). Coupling constants J were reported in Hz to the nearest 0.01 Hz. Peak multiplicity was indicated as follows s (singlet), d (doublet), t (triplet), q (quartet), m (multiplet), br (broad signal) ad (apparent doublet) and aq (apparent quartet). ESI-MS were recorded on LC-MS LCQ Fleet ThermoFisher Scientific. UV–vis spectra were recorded on BMG Labtech Spectrostar Nano using a 1 cm quartz cell or a 96 well plate. Fluorescence spectra were registered on a HORIBA FluoroMax Plus spectrofluorimeter using 1.0 cm cell. Flash chromatography was performed on Merk silica gel 60 (0.040–0.063 mm). The thin layer chromatography was performed on Supelco TLC Silica gel 60 F254 (aluminum sheets or glass plates). High resolution mass analyses were acquired with a resolution of 70000 FWHM at m/z= 200 in

View Article Online
DOI: 10.1039/D5CB00190K

an alternate electrospray mode with data-dependent acquisition of HCD fragmentation spectra (resolution 17500 FWHM at m/z=200) of the more abundant monocharged ions (Q-Exactive hybrid quadrupole – orbitrap mass analyzer, Thermo Scientific).

Synthesis of 6. Tris-BODIPY-OH (23 mg, 0.026 mmol) was suspended in DCM (1.15 mL), then pyridine (28 µL, 0.35 mmol), chloroacetic anhydride (60 mg, 0.35 mmol) and DMAP (0.95 mg, 7.8 x 10^{-3} mmol) were added. The reaction mixture was stirred at r.t. for 24 h, then it was diluted with dichloromethane (100 mL) and washed with a saturated solution of ammonium chloride (3 x 10 mL), and with brine (1 x 10 mL). The organic phase was dried with Na_2SO_4, filtered, and concentrated under vacuum to give **6** (38 mg, 94%) as a reddish glassy solid. ESI-MS: calcd. for $C_{61}H_{64}BCl_9F_2N_5O_{21}^-$ $[M\text{-}H^+]^-$ 1566.14 found 1566.47. ^{1}H NMR (400 MHz, $CDCl_3$) δ: 8.12 (s, 1H), 8.00 – 7.99 (m, 2H), 7.49 – 7.47 (m, 2H), 4.72 (s, 2H), 4.35 (s, 4H), 4.28 (s, 6H), 4.25 (s, 12H), 4.06 (s, 6H), 4.03 (s, 12H), 3.63 (s, 2H), 3.57 (s, 4H), 2.64 (s, 6H,), 1.52 (s, 6H).^{13}C-NMR (101 MHz, $CDCl_3$) δ: 166.8, 166.8, 159., 145.5, 144.7, 140.8, 137.7, 134.7, 130.8, 129.6, 121.2, 120.9, 115.6, 91.6, 78.8, 68.0, 67.4, 64.6, 64.0, 63.8, 59.6, 43.2, 43.0, 40.7, 40.6, 13.8.

Synthesis of Man$_9$-BODIPY. In a Schlenk flask vial, **6** (17.3 mg, 0.011mmol) was dissolved in dry DMF (0.5 mL), then sodium iodide (33 mg, 0.22 mmol) was added and the mixture degassed with three cycles of *vacuum*-argon. In a second flask, **1** (36 mg, 0.15 mmol) was dissolved into dry DMF (0.5 mL) and degassed with three cycles of *vacuum*-argon. Then, the solution of α-mannoside **1** and dry DIPEA (105 µL, 0.605 mmol) were added to the solution of BODIPY **6**. The reaction mixture was stirred at r.t.. The reaction progression was monitored by C18 modified silica thin layer chromatography (acetonitrile:water 1:1). After the complete consumption of BODIPY **6** (19 h), the solvent was removed under vacuum and the solid washed with Et_2O (5 x 2 mL) and DCM (5 x 2 mL). Then the crude was dissolved in milliQ water (2 mL) and dialyzed *vs* water (MWCO 1000 Da, 1L milliQ water, replaced every 8 h) for 24 h. Then the solution was freeze-dried affording **Man$_9$-BODIPY** (33.6 mg, 89%) as a highly hygroscopic fluffy solid.^{1}H NMR (400 MHz, D_2O) δ: 8.37 (bs, 1H), 7.82 (bs, 2H), 7.13 (bs, 2H), 4.77 – 4.66 (m, 11H), 4.22 (bs, 4H), 4.03 (bs, 17H), 3.82 – 3.37 (m, 76H), 3.24 – 3.19 (m, , 9H), 2.65 (d, *J* = 17.1 Hz, 16H), 2.33 (bs, 6H), 1.27 (bs, 6H). ^{13}C-NMR (101 MHz, D_2O, 60°C) δ: 171.7, 171.5, 146.1, 144.9, 141.6, 137.9, 134.4, 131.0, 122.2, 121.3, 100.3, 100.2, 93.5, 78.8, 73.3, 71.2, 70.5, 67.1, 66.8, 64.0, 61.3, 43.5, 43.3, 33.9, 32.2, 13.8. HR-MS: calcd. for $C_{133}H_{202}BF_2N_5O_{75}S_9$ $[M+2H]^{2+}$ 1703.9864 found 1703.9869 Δ = -0.24 ppm.

View Article Online
DOI: 10.1039/D5CB00190K

Synthesis of (Man-TEG)$_9$-BODIPY. In a Schlenk flask, **6** (23.2 mg, 0.015mmol) was dissolved in dry DMF (0.75 mL), then sodium iodide (45 mg, 0.3 mmol) was added and the mixture degassed with three cycles of *vacuum*-argon. In a second flask, α-mannoside **2** (65.8 mg, 0.2 mmol) was dissolved into dry DMF (0.75 mL) and degassed with three cycles of *vacuum*-argon. Then, the solution of **2** and dry DIPEA (143 µL, 0.825 mmol) were added to the solution of BODIPY **6**. The reaction mixture was stirred at r.t.. The reaction progression was monitored by C18 modified silica thin layer chromatography (acetonitrile:water 1:1). After the complete consumption of BODIPY **6** (19 h), the solvent was removed under vacuum and the solid washed with Et_2O (5 x 2 mL) and DCM (5 x 2 mL). Then the crude was dissolved in milliQ water (2 mL) and dialyzed *vs* water (MWCO 1000 Da, 1L milliQ water, replaced every 8 h) for 24 h. Then the solution was freeze-dried affording **(Man-TEG)$_9$-BODIPY** (42.0 mg, 69%) as a highly hygroscopic fluffy solid. ^{1}H NMR (400 MHz, D_2O) δ: 8.50 (bs, 1H), 7.95 (bs, 2H), 7.31 (bs, 2H), 4.81 (bs, 16H), 4.14 (bs, 36H), 3.98 – 3.06 (m, 30H), 2.71 (s, 30H), 2.47 (s, 5H), 0.73 (s, 5H). ^{13}C-NMR (101 MHz, D_2O, 60°C) δ: 171.7, 100.4, 100.3, 73.2, 71.1, 70.53, 70.46, 70.1, 70.0, 67.2, 66.8, 63.9, 61.4, 61.3, 43.3, 33.8, 32.1, 23.7, 23.2, carbons of the BODIPY were not visible in these conditions. HR-MS: calcd. for $C_{169}H_{274}BF_2N_5O_{75}S_9$ $[M+2H]^{2+}$ 2098.72188 found 2098.71997, δ = -0.91 ppm.

C-type lectins-Fc: DC-SIGN-Fc consists of the extracellular portion of DC-SIGN fused to a human IgG1-Fc fragment.[37] Langerin-Fc was generated by amplifying RNA encoding the extracellular domains of langerin and fused to human IgG1-Fc.[38]

Turbidimetry analysis. The agglutination assay was carried as reported in the literature with minor modifications.[28] **Tris-BODiPY-OH**, **Man$_9$-BODIPY** and **(Man-TEG)$_9$-BODIPY** were first dissolved in DMSO (1 mM), then the BODIPY solutions were diluted to 20 µM in the buffer (HEPES 25 mM pH 7.6, 1 mM $CaCl_2$, 1 mM $MnCl_2$). A solution of ConA (20 µM) in the buffer (HEPES 25 mM pH 7.6, 1 mM $CaCl_2$, 1 mM $MnCl_2$) was prepared. In a 96-well plate (Microplate, 96 wells, PS, F-BOTTOM (CHIMNEY WELL), clear, non-binding) were placed 100 µL of the 20 µM solution of each BODIPY, then 100 µL of the solution of ConA were added. The mixture was gentle shacked for 10 minutes, then the optical density at $\lambda = 490$ nm was measured every minute for 30 minutes. The measurements were carried out in triplicate. Deagglutination was performed by adding a solution of α-*O*-methyl-D-mannopyranoside directly in the 96-wells plate to reach 50 mM concentration in the well and monitoring the decrease of the optical density at $\lambda = 490$ nm.

View Article Online
DOI: 10.1039/D5CB00190K

Fluorescence lifetime imaging (FLIM). FLIM was performed at room temperature (20 °C) on a Nikon Ti AX-R NSPARC confocal microscope using a Nikon Plan Apo λD 100x oil immersion objective (NA = 1.45). The microscope is equipped with a two channel PicoQuant FLIM compact module system. Images of 1024x1024 pixels were acquired using a 488nm pulsed laser for excitation and recording photons of fluorescence emission with wavelength 620 $\pm$ 50 nm for 90s at a frequency of 25MHz through a PMA Hybrid single photon counting module and a MultiHarp 150 multichannel event timer. Lifetime histograms were calculated and analyzed using SymphoTime©. Samples were inserted into LabteK chambers, and the images were acquired at 10 μm from the coverslip to avoid interactions of the dye with the surface of the coverslip. Sample preparation: 1 mM stock solutions of **Tris-BODIPY-OH**, **Man$_9$-BODIPY** and **(Man-TEG)$_9$-BODIPY** in pure DMSO were prepared and later diluted to 500nM in HEPES 25 mM, 1 mM $CaCl_2$, 1 mM $MnCl_2$ buffer (pH = 7.6); FLIM was performed on the 500 nM solution of each dye in absence or presence of 500 nM Con A.

Fluorescence polarization (FP). Fluorescence polarization assays were performed using a Tecan Spark multimode microplate reader (Tecan Trading AG, Switzerland), where a fluorescence polarization of BODIPY probes **Tris-BODIPY-OH**, **Man$_9$-BODIPY** and **(Man-TEG)$_9$-BODIPY** was measured by excitation at 520/15 nm and emission at 555/15 nm. 1 mM stock solutions of **Tris-BODIPY-OH**, **Man$_9$-BODIPY** and **(Man-TEG)$_9$-BODIPY** were prepared in pure DMSO and later diluted in the buffer (HEPES 25 mM, 1 mM $CaCl_2$, 1 mM $MnCl_2$, pH = 7.6) to the final concentration of 1 µM. Concanavalin A (ConA) was dissolved in the same buffer and 100 µM stock solution was prepared, which was later diluted to 40 µM. ConA (20 µM-0.078 µM) was titrated against a fixed concentration of **Tris-BODIPY-OH**, **Man$_9$-BODIPY** and **(Man-TEG)$_9$-BODIPY** (0.5 µM). All experiments were performed at room temperature (25 °C).

Competitive fluorescence polarization assay. Fixed concentrations of **Man$_9$-BODIPY** (0.5 µM) and ConA (2 µM) were used in a competitive fluorescence polarisation assay. The highest D-mannose concentration was 100 mM and the lowest 190 µM. All experiments were performed at room temperature (25 °C).

Fluorescence correlation spectroscopy (FCS). 1 mM stock solutions of **Tris-BODIPY-OH** and **Man$_9$-BODIPY** in pure DMSO were prepared and later diluted in HEPES 25 mM, 1 mM $CaCl_2$, 1 mM $MnCl_2$ buffer (pH = 7.6). 500 nM solution of each dye in absence or presence of 50 nM ConA was placed in glass-bottom ibidi 18-well µslides, precoated with albumin (Sigma Aldrich) to reduce dye adsorption to the surface. FCS experiments were

View Article Online
DOI: 10.1039/D5CB00190K

performed with an Abberior Instruments microscope in the confocal mode using the Olympus UPlanSApo 60x/1.2 water immersion objective and steered through the Imspector software. Fluorescence was excited by a 561-nm pulsed excitation laser at average power around 10 μW, and detected by an avalanche photodiode through a 0.9 Airy-unit pinhole and a 580–630 nm emission filter (Semrock). Intensity fluctuations were acquired in 2 μs bins for 15–120 seconds at least 5 times per sample. The intensity traces were autocorrelated and further analysed with the open source FoCuS-scan software (https://github.com/dwaithe/FCS_scanning_correlator)[41] employing the 3D-diffusion model (fits in **Figure 8**) with the aspect ratio of the optical point-spread-function and anomalous diffusion exponent fixed to 10 and 0.9, respectively. The obtained transit times (**Figure S17A**) were transformed into diffusion coefficients (**Figure S17B**) according to the measurements of the reference probe Rhodamine B with known diffusion coefficient.[42] For data for the samples with ConA were fit with a two-component model describing two diffusing species – the free probe (parameters fixed to the values obtained for that probe alone), and bound probe (fraction displayed in **Figure S17C**).

Acknowledgement

The financial support of this work from the Slovenian Research Agency (Grant P1-0208; P1-0060) is gratefully acknowledged. This research was supported by the Ministry of Education, Science, and Sport (MIZŠ) of the Republic of Slovenia and the European Regional Development Fund OP20.05187 RI-SI-EATRIS. We also thank Eva Cerkvenik for her assistance in the lab during FCS measurements. GB, JT, SC and BR thank ("Progetto Dipartimenti di Eccellenza 2013–2027", allocated to Department of Chemistry "Ugo Schiff"). B.R. thanks L'Amore di Matteo Coveri ONLUS for financial support. S. C. thanks the support of the European Union by the Next Generation EU project ECS00000017 'Ecosistema dell'Innovazione' Tuscany Health Ecosystem (THE, PNRR, Spoke 4: Nanotechnologies for diagnosis and therapy). ML acknowledges financial support from the European Union - NextGeneration EU, DM 737/2021, "bando IR@Unifi2023", Project code HIRES, CUP B55F21007810001, and "Progetto PNRR_CN3_RNA_Spoke_5 - PNRR_CN 3_Centro Nazionale di Ricerca Sviluppo di terapia genica e farmaci con tecnologia a RNA", CUP B13C220010100012.

View Article Online
DOI: 10.1039/D5CB00190K

Conflict of interest

There are no conflicts to declare.

Data availability

The data supporting this article have been included as part of the Supplementary Information.

Author Contributions

G.B. (Data curation: Lead; Formal analysis: Lead; Investigation: Lead; Validation: Lead; Visualization: Lead); E.P. (Data curation: Lead; Formal analysis: Lead; Investigation: Lead; Validation: Lead; Visualization: Lead); J.T. (Data curation: Equal; Formal analysis: Equal; Investigation: Equal; Validation: Equal; Visualization: Equal); J.M. (Data curation: Equal; Formal analysis: Equal; Investigation: Equal; Validation: Equal; Visualization: Equal); S.C. (Funding acquisition: Equal; Methodology: Supporting; Visualization: Supporting; Writing – review & editing: Supporting); M.L. (Methodology: Equal; Investigation: Lead; Resources: Equal; Writing – review & editing: Equal); Y.K. (Methodology: Supporting; Resources: Lead; Writing – review & editing: Supporting); F.C. (Methodology: Equal; Resources: Equal; Writing – review & editing: Supporting); I.U. (Methodology: Equal; Resources: Equal; Supervision: Lead; Writing – review & editing: Equal); M.A. (Funding acquisition: Lead; Methodology: Lead; Resources: Lead; Supervision: Lead; Visualization: Equal; Writing – original draft: Lead; Writing – review & editing: Lead); B.R. (Conceptualization: Lead; Funding acquisition: Lead; Methodology: Lead; Project administration: Lead; Resources: Lead; Supervision: Lead; Visualization: Lead; Writing – original draft: Lead; Writing – review & editing: Lead).

References

1 A. Barattucci, C. M. A. Gangemi, A. Santoro, S. Campagna, F. Puntoriero and P. Bonaccorsi, *Org. Biomol. Chem.*, 2022, **20**, 2742–2763.

2 A. M. Gomez and J. C. Lopez, *Chem. Rec.*, 2021, **21**, 3112–3130.

3 S.-H. Son, S. Daikoku, A. Ohtake, K. Suzuki, K. Kabayama, Y. Ito and O. Kanie, *Chem. Commun.*, 2014, **50**, 3010–3013.

View Article Online
DOI: 10.1039/D5CB00190K

4 K. Arai, A. Ohtake, S. Daikoku, K. Suzuki, Y. Ito, K. Kabayama, K. Fukase, Y. Kanie and O. Kanie, *Org. Biomol. Chem.*, 2020, **18**, 3724–3733.

5 J. Sibold, K. Kettelhoit, L. Vuong, F. Liu, D. B. Werz and C. Steinem, *Angew. Chemie Int. Ed.*, 2019, **58**, 17805–17813.

6 N. Shivran, M. Tyagi, S. Mula, P. Gupta, B. Saha, B. S. Patro and S. Chattopadhyay, *Eur. J. Med. Chem.*, 2016, **122**, 352–365.

7 Q. Zhang, Y. Cai, Q. Li, L. Hao, Z. Ma, X. Wang and J. Yin, *Chem. – A Eur. J.*, 2017, **23**, 14307–14315.

8 G. Biagiotti, E. Purić, I. Urbančič, A. Krišelj, M. Weiss, J. Mravljak, C. Gellini, L. Lay, F. Chiodo, M. Anderluh, S. Cicchi and B. Richichi, *Bioorg. Chem.*, 2021, **109**, 104730.

9 G. E. Giacomazzo, P. Palladino, C. Gellini, G. Salerno, V. Baldoneschi, A. Feis, S. Scarano, M. Minunni and B. Richichi, *RSC Adv.*, 2019, **9**, 30773–30777.

10 A. Bernardi, J. Jiménez-Barbero, A. Casnati, C. De Castro, T. Darbre, F. Fieschi, J. Finne, H. Funken, K.-E. Jaeger, M. Lahmann, T. K. Lindhorst, M. Marradi, P. Messner, A. Molinaro, P. V Murphy, C. Nativi, S. Oscarson, S. Penadés, F. Peri, R. J. Pieters, O. Renaudet, J.-L. Reymond, B. Richichi, J. Rojo, F. Sansone, C. Schäffer, W. B. Turnbull, T. Velasco-Torrijos, S. Vidal, S. Vincent, T. Wennekes, H. Zuilhof and A. Imberty, *Chem. Soc. Rev.*, 2013, **42**, 4709–27.

11 L. Baldini, A. Casnati and F. Sansone, *European J. Org. Chem.*, 2020, **2020**, 5056–5069.

12 D. Pagé and R. Roy, *Bioconjug. Chem.*, 1997, **8**, 714–723.

13 J. I. Quintana, U. Atxabal, L. Unione, A. Ardá and J. Jiménez-Barbero, *Chem. Soc. Rev.*, 2023, **52**, 1591–1613.

14 D. Goyard, A. M.-S. Ortiz, D. Boturyn and O. Renaudet, *Chem. Soc. Rev.*, 2022, **51**, 8756–8783.

15 M. Martínez-Bailén, J. Rojo and J. Ramos-Soriano, *Chem. Soc. Rev.*, 2023, **52**, 536–572.

16 M. C. Galan, P. Dumy and O. Renaudet, *Chem. Soc. Rev.*, 2013, **42**, 4599–4612.

17 K. G. Leslie, S. S. Berry, G. J. Miller and C. S. Mahon, *J. Am. Chem. Soc.*, 2024, **146**, 27215–27232.

18 R. J. Pieters, *Org. Biomol. Chem.*, 2009, **7**, 2013–25.

19 A. Imberty, Y. M. Chabre and R. Roy, *Chem. – A Eur. J.*, 2008, **14**, 7490–7499.

20 J. J. Lundquist and E. J. Toone, *Chem. Rev.*, 2002, **102**, 555–578.

21 J. Tricomi, G. Biagiotti, T. Chastel, S. Filiberti, H. Kokot, F. Mancusi, M. Žežlina, L. Rajeh, I. Urbančič, S. Bodin, E. G. Occhiato, A. Turtoi, S. Cicchi and B. Richichi, *ACS Bio Med Chem Au*, 2025, **5**, 895–905.

22 C. Grandjean, H. Gras-Masse and O. Melnyk, *Chem. - A Eur. J.*, 2001, **7**, 230–239.

23 M. A. Hollas, S. J. Webb, S. L. Flitsch and A. J. Fielding, *Angew. Chemie - Int. Ed.*, 2017, **56**, 9449–9453.

24 N. A. Uhlich, T. Darbre and J.-L. Reymond, *Org. Biomol. Chem.*, 2011, **9**, 7071–84.

25 G. Michaud, R. Visini, M. Bergmann, G. Salerno, R. Bosco, E. Gillon, B. Richichi, C. Nativi, A. Imberty, A. Stocker, T. Darbre and J.-L. Reymond, *Chem. Sci.*, 2016, **7**, 166–182.

26 E. C. Stanca-Kaposta, D. P. Gamblin, E. J. Cocinero, J. Frey, R. T. Kroemer, A. J. Fairbanks, B. G. Davis and J. P. Simons, *J. Am. Chem. Soc.*, 2008, **130**, 10691–10696.

27 A. Meyer, M. Noël, J. Vasseur and F. Morvan, *European J. Org. Chem.*, 2015, **2015**, 2921–2927.

28 S. Schmid, A. Mishra, M. Wunderlin and P. Bäuerle, *Org. Biomol. Chem.*, 2013, **11**, 5656–65.

29 R. Datta, T. M. Heaster, J. T. Sharick, A. A. Gillette and M. C. Skala, *J. Biomed. Opt.*, 2020, **25**, 1–43.

30 M. D. Hall, A. Yasgar, T. Peryea, J. C. Braisted, A. Jadhav, A. Simeonov and N. P. Coussens, *Methods Appl. Fluoresc.*, 2016, **4**, 022001.

31 R. V. Weatherman, K. H. Mortell, M. Chervenak, L. L. Kiessling and E. J. Toone, *Biochemistry*, 1996, **35**, 3619–3624.

32 R. V. Weatherman and L. L. Kiessling, *J. Org. Chem.*, 1996, **61**, 534–538.

View Article Online
DOI: 10.1039/D5CB00190K

33 E. L. Elson, *Biophys. J.*, 2011, **101**, 2855–2870.

34 I. Urbančič, B. C. Lagerholm and F. Schneider, in *Imaging Modalities for Biological and Preclinical Research: A Compendium, Volume 1: Part I: Ex vivo biological imaging*, IOP Publishing, 2021.

35 T. B. H. Geijtenbeek and S. I. Gringhuis, *Nat. Rev. Immunol.*, 2009, **9**, 465–479.

36 G. D. Brown, J. A. Willment and L. Whitehead, *Nat. Rev. Immunol.*, 2018, **18**, 374–389.

37 T. B. H. Geijtenbeek, G. C. F. van Duijnhoven, S. J. van Vliet, E. Krieger, G. Vriend, C. G. Figdor and Y. van Kooyk, *J. Biol. Chem.*, 2002, **277**, 11314–11320.

38 C. M. Fehres, S. Duinkerken, S. C. Bruijns, H. Kalay, S. J. van Vliet, M. Ambrosini, T. D. de Gruijl, W. W. Unger, J. J. Garcia-Vallejo and Y. van Kooyk, *Cell. Mol. Immunol.*, 2017, **14**, 360–370.

39 B. Belardi and C. R. Bertozzi, *Chem. Biol.*, 2015, **22**, 983–993.

40 E. Zahorska, L. M. Denig, S. Lienenklaus, S. Kuhaudomlarp, T. Tschernig, P. Lipp, A. Munder, E. Gillon, S. Minervini, V. Verkhova, A. Imberty, S. Wagner and A. Titz, *JACS Au*, 2024, **4**, 4715–4728.

41 D. Waithe, F. Schneider, J. Chojnacki, M. P. Clausen, D. Shrestha, J. B. de la Serna and C. Eggeling, *Methods*, 2018, **140**–**141**, 62–73.

42 Kapusta P 2010 PicoQuant Application Note: Absolute Diffusion Coefficients: Compilation of Reference Data for FCS Calibration, https://picoquant.com/images/uploads/page/files/%0A7353/appnote_diffusioncoefficients.pdf.

A nonavalent BODIPY with a multivalent arrangement of α-mannosides enables lectins recognition in fluorescence-based assays

Giacomo Biagiotti,[a,§] Edvin Purić,[b,§] Jacopo Tricomi,[a] Janez Mravljak,[b] Stefano Cicchi,[a] Marco Laurati,[a,f] Yvette van Kooyk,[c] Fabrizio Chiodo,[c,d] Iztok Urbančič,[e] Marko Anderluh,[b,*] Barbara Richichi[a,*]

[a]*Department of Chemistry 'Ugo Schiff', University of Firenze, Via della Lastruccia 3-13, 50019 Sesto Fiorentino, Italy*
[b]*Department of Pharmaceutical Chemistry, Faculty of Pharmacy, University of Ljubljana, Aškerčeva cesta 7, 1000 Ljubljana, Slovenia*
[c]*Department of Molecular Cell Biology and Immunology, Amsterdam UMC, Vrije Universiteit Amsterdam, Amsterdam 1081 HV, The Netherlands.*
[d]*Institute of Biomolecular Chemistry, National Research Council (CNR), via Campi Flegrei, 34, 80078 Pozzuoli, Naples, Italy.*
[e]*Laboratory of Biophysics, Condensed Matter Physics Department, Jožef Stefan Institute, Jamova Cesta 39, Ljubljana, Slovenia*
[f] *Consorzio per lo Sviluppo dei Sistemi a Grande Interfase, 50019 Sesto Fiorentino (FI), Firenze, Italy*
E-mail: barbara.richichi@unifi.it

Marko.Anderluh@ffa.uni-lj.si

§ G.B. and E.P. equally contributed to this work

Data availability statements

The data supporting this article have been included as part of the Supplementary Information.